Bloch Oscillating Super-Superlattices

P Robrish[a], J Xu[b], S Kobayashi[c,d], P G Savvidis[c], B Kolasa[b], G Lee[a], D Mars[a] and S J Allen[b,c]

[a] Agilent Laboratories, Palo Alto,
[b]UCSB,Physics Dept., Santa Barbara
[c]UCSB, Institute for Quantum and Complex Dynamics, Santa Barbara,
[d]The University of Tokyo, Institute of Industrial Science, Tokyo

Abstract. Bloch oscillation in electrically biased semiconductor superlattices offers broadband terahertz gain from DC up to the Bloch frequency and can provide a basis for solid-state electronic oscillators operating at 10 times the frequency of existing devices. To circumvent the inherent instability of the electrically biased doped superlattices to the formation of static or dynamic electric field domains, we have fabricated super-superlattices in which a large superlattice is punctuated with heavily doped regions. Room temperature, terahertz photon assisted transport in short InGaAs/InAlAs superlattice cells allows us to determine the Stark ladder splitting as the superlattice is electrically biased and confirms the absence of electric field domains in short structures. Absorption of radiation from 1.5 to 2.5 THz by electrically biased InAs/AlSb super-superlattices exhibit a crossover from loss to gain as the Stark ladder is opened.

1. Introduction

The terahertz part of the electromagnetic spectrum is marked by a lack of commercial technology. This is readily apparent if we focus on fundamental solid-state oscillators or sources, Figure 1. On the electronic end the technology drive has pushed quantum transport devices like resonant tunneling diodes but the most effective solid state sources of terahertz radiation are harmonic generators [1]. On the photonic end the most impressive gains are made by the development of long wavelength quantum cascade lasers (QCL's), [2,3].

Bloch oscillating superlattices have the potential to provide broad band gain at terahertz frequencies and may be the basis of a technology that will help fill the gap in solid state terahertz fundamental oscillators. The seminal work of Esaki and Tsu [4] drew attention to the fact that the relatively large scale periodic structures in semiconductor superlattices made them ideal solids in which to explore and use Bloch oscillation. Following this work, which predicted that electrically biased semiconductor superlattices will exhibit negative differential conductivity (NDC) [4] like the Gunn effect, Ktitorov et al showed theoretically that the negative resistance and potential gain should persists up the Bloch frequency or spacing between the rungs of the Stark ladder [5]. Unlike the Gunn

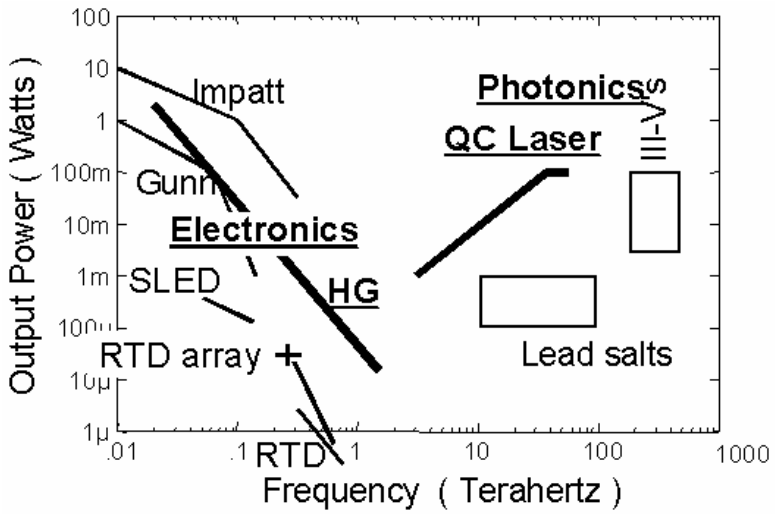

Figure 1. The terahertz technology landscape. The low frequency end of the terahertz spectrum engages electronic transport devices; the high frequency end photonic quantum transition devices.

effect which persists only up to the energy relaxation rate, 100-200 GHz, electrically biased semiconductor superlattices should exhibit gain over a much larger band width, up to several terahertz. See Figure 2. [6]

2. Stabilizing the electric field.

It is well known that a medium with bulk negative differential conductivity (NDC) exhibits space charge instabilities, which lead to electric field domains and current self-oscillations [7 , 8]. But, if the material is sufficiently short, small space charge fluctuations that could grow and provide electric field domain walls are swept out before a domain wall is established. As in the Gunn effect, we can define a critical "nL" product below which propagating electric field domains are suppressed. Here, n is the electron density and L is the sample length.

For a semiconductor superlattice we estimate that if $nL < 7\varepsilon E_c / e$, where ε is the dielectric permittivity and E_c the the critical field at which NDC sets in, space charge instabilities are swept out of the superlattice before they form a domain wall [9,10]. For superlattice doping densities of the order of 2.5 – 5.0 10^{16} $cm^{-3,}$ and critical fields of the order of ~ 6 kV/cm, critical lengths are of the order of 100-200 nm. For superlattice periods of 10 nm this requires lengths less than 10-20 quantum wells, very short superlattices indeed.

On the other hand to mitigate the effects of parasitic contact resistance, shunt capacitance and to ultimately deliver useful power, long superlattices, of the order of 5-10 μm are needed. To satisfy both requirements, short superlattices and long devices, we fabricate super-superlattices comprised of a stack of short superlattices, each short section separated from its neighbours by a heavily doped region. (Figure 2)

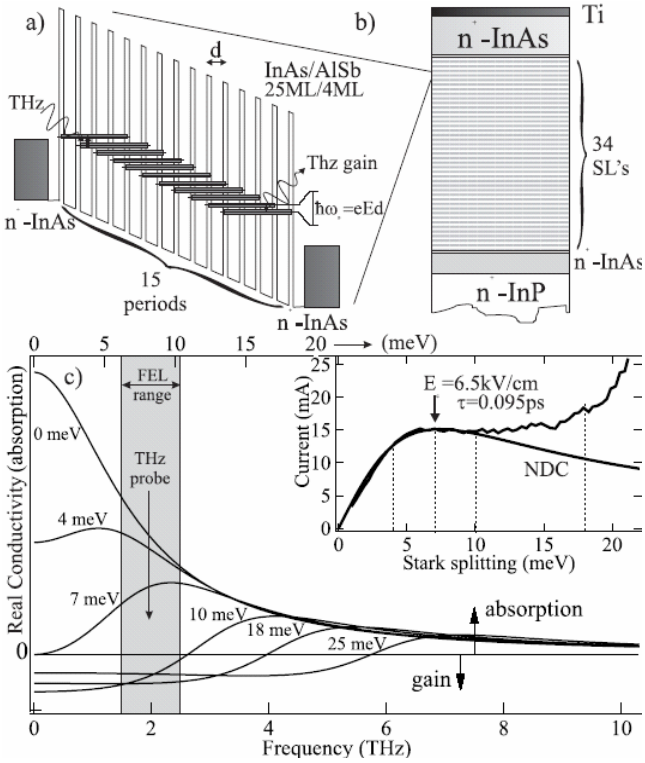

Figure 2. (a) A superlattice structure under electrical bias. (b) A stack of short superlattice cells. Lower: The differential conductance is expected to be suppressed and exhibit negative conductance up to the Bloch frequency of Stark ladder spacing. From Ref. 6.

3. Stark ladder spectroscopy

To experimentally confirm the notion that short superlattice sections will sustain a stable and reasonably uniform electric field, terahertz photon assisted transport measurements were performed on various test structures. These consisted of short superlattices (cells) of either 9 or 15 quantum wells sandwiched between n^+ regions. Samples were tested that contained stacks of 1, 2 or 5 of these cells. 18 or 14 μm diameter mesas were etched and the chip mounted and bonded at the end of an SMA connector. Special electronics measured the current-voltage (I-V) characteristic of the device under test (DUT) on a time scale of the order of ~1 μsec. In this manner the entire I-V could be measured while the several microsecond long terahertz radiation from the UCSB free-electron lasers was focused on the device.

Figure 3 shows the differential conductance, dJ/dV, of a terahertz irradiated 2 cell stack. Here each cell consists of a 15 quantum well, InGaAs/InAlAs, superlattice. A peak in differential conductance appears at a voltage that depends on frequency. In essence, when the spacing of the rungs of the Stark ladder exceeds the terahertz photon energy the electrons are driven down the ladder, causing an increase in current (positive dJ/dV), feeding energy into the radiation field (the gain channel). [11,12]

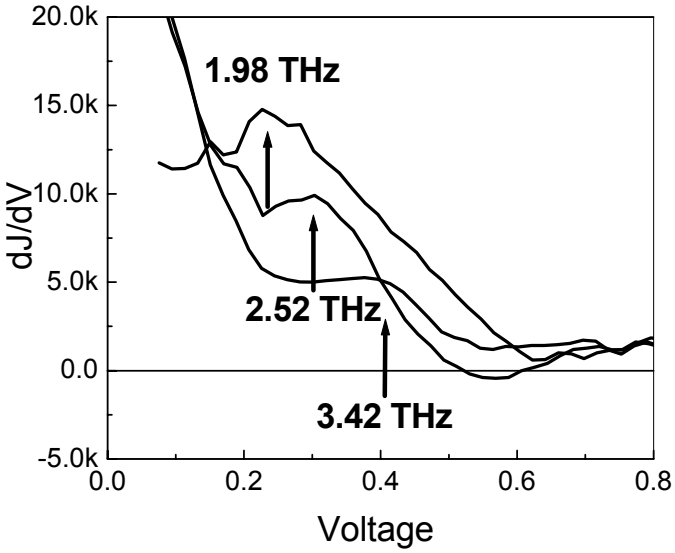

Figure 3. The terahertz irradiated differential conductance, dJ/dV, of a 2 cell stack. Each cell consists of a 15 quantum well, InGaAs/InAlAs, superlattice. A peak in differential conductance appears at a voltage that depends on frequency.

A quantitative description of this phenomenon follows much earlier developments of microwave photon assisted transport in superconducting junctions. [13] The DC current flow in the presence of a DC voltage and strong terahertz field may be expressed as [14]

$$I(V) = \sum_{n=-\infty}^{\infty} J_n^2\left(eaE_{THz}/\hbar\omega\right)\cdot I_0\left(V + n\hbar\omega/e\right)$$

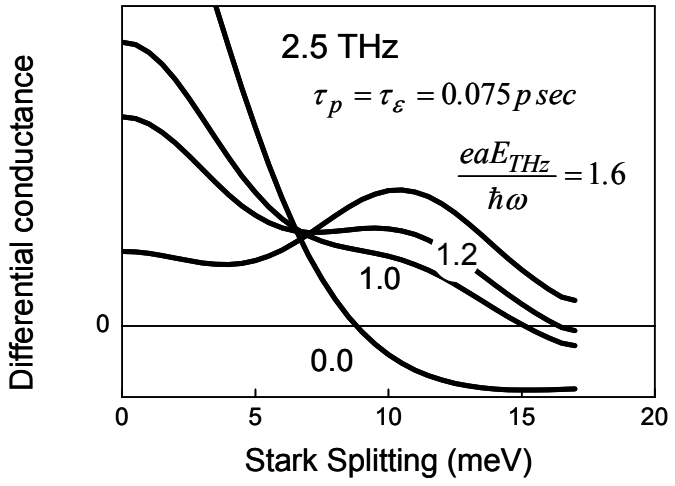

Figure 4. Model calculation of differential conductance with terahertz field strength as a parameter.

where V is the applied DC voltage, J_n, the n-th order Bessel function, I, the current, and I_0 the current in the absence of terahertz radiation. The superlattice period is a, the strength of the terahertz field E_{THz} at frequency ω. $\hbar$ and e are Planck's constant and the electron

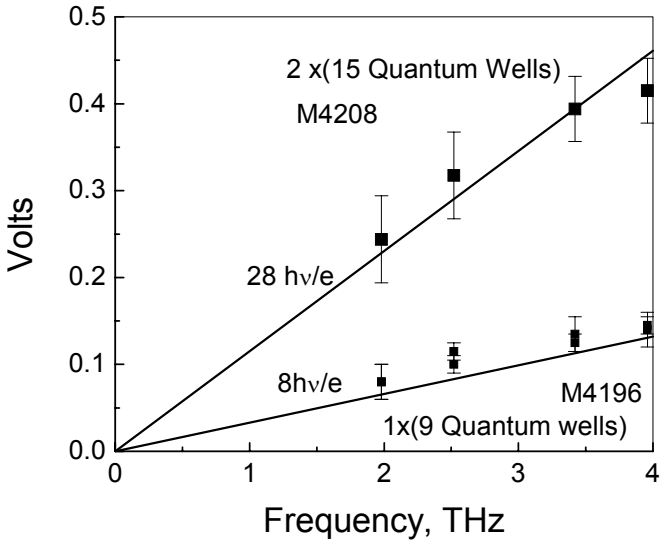

Figure 5. Voltage bias at differential conductance maxima vs. terahertz frequency. Upper data: 1 stacked 15 quantum well cells. Lower data: a single cell of 9 quantum wells.

charge. Figure 3 and Figure 4 may be compared, extracting an estimate of the internal terahertz field strength. More important the comparisons quantitatively support the notion that the peak in differential conductance corresponds to resonance of the terahertz radiation and Stark ladder rung spacing.

Figure exhibits the voltage of the differential conductance maxima vs. terahertz frequency. The solid lines correspond to the expected voltage vs. frequency if the voltage were uniformly dropped across the superlattice sections. We note here that there are (n-1) separations for n quantum wells in a single cell.

4. Loss and Gain under Electrical Bias

Experimentally, photon assisted transport proceeds in a relatively straight forward manner; the sample is the detector. Details concerning coupling of the terahertz radiation to the sample are not important provide that enough power is available and the desired changes in differential conductance appear.

Measurement of the dynamical conductance, which is directly related to "loss and gain" in electrically biased superlattices is more difficult. Here, we load a terahertz waveguide with a row of super-superlattices and measure the transmission through the waveguide as a function of electrical bias.

The wave guide is formed by etching the superlattice wafer as shown in Figure . The n^+ substrate forms the bottom of the waveguide and metal gold plated brass the top. A hole in the top of the guide directs the transmitted terahertz radiation to a detector.

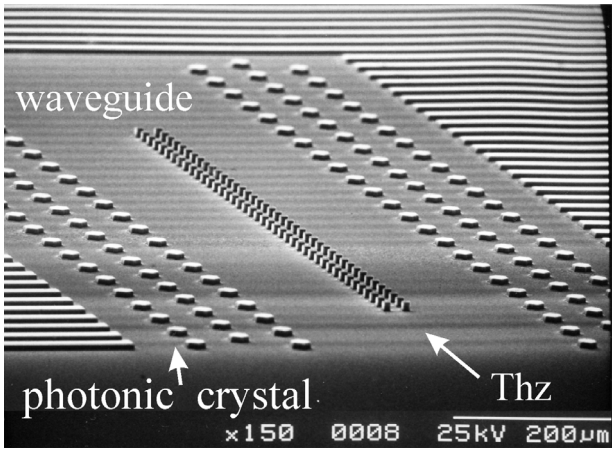

Figure 6. Terahertz waveguide with metallic top removed. The sidewalls are defined by a photonic bandgap structure. Radiation enters the 10 μm high waveguide and exits through a hole in the metallic top and is directed to a detector.

Transmission is measured as a function of electrical bias applied to the row of super-superlattice mesas in the center of the guide.

Transmission measurements were carried out at frequencies between 1.5 and 2.5 THz (Figure 2). Figure shows the change in transmission vs. voltage at 1.98 THz. [6] The voltage required to open the transmission through the guide is about 80% of that expected which implies that ~ 20% of the superlattice experience little or no field. This result is obtained at each frequency between 1.5 and 2.5 THz. (Figure) The voltage required to open the transmission is proportional to frequency but ~75-80% of that expected.

Unlike the test structures used for the Stark ladder spectroscopy, here there was no "set back" region between the n^+ and short superlattice. Spill over from the heavily doped

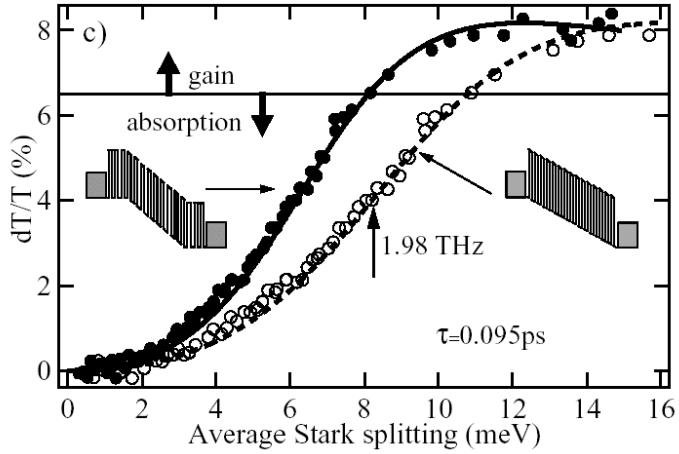

Figure 7. Fractional change in transmission vs. applied voltage expressed as average Stark ladder splitting. Solid points are the data; open circles expected voltage dependence.

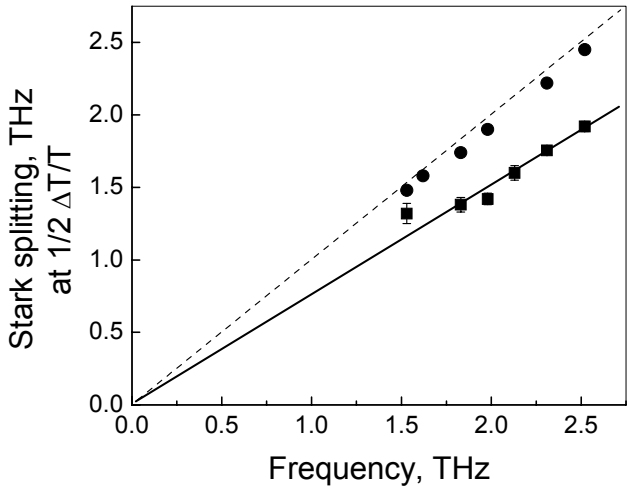

Figure 8. Voltage at differential conductance maxima vs. applied THz frequency. Upper trace is the expected voltage at the 1/2 'power" point of the loss /gain cross over expressed as the average Stark splitting. The lower trace is measured. It requires ~80% of the expected voltage to open the requisite Stark ladder splitting. [6]

region may effectively "short-circuit" several quantum wells at the edges of the superlattice producing the result shown in Figure .

5. Conclusions

Stark ladder spectroscopy by terahertz photon assisted transport and terahertz waveguide measurements of the bias dependence dynamical conductance, indicate that short period superlattices can be used to achieve essentially uniform electric fields. While the field distribution of sub critical bulk negative resistance material should have no static or dynamic domains, the field is not expected to be entirely uniform. But the gain band width of these materials are expected to be very broad (Figure 2) and modestly slow varying electric fields will be of little consequence. But the Stark ladder spectroscopy directly speaks to this issue and it is apparent that for the range of fields and doping presented here the field distribution is quite uniform.

Acknowledgements: Work at UCSB was supported by the ARO, DARPA/ONR and CNID.

References

[1] Weikle R M, II, Crowe T W, Kollberg E L 2003 Inter. J. of High Speed Electronics & Systems 13 429
[2] Kohler R, Tredicucci A, Beltram F, Beere H E, Linfield E H, Davies A G, Ritchie D A 2002 Appl. Phys. Lett. 80 1867
[3] Williams B S, Kumar S, Callebaut H, Qing Hu, Reno J H 2003 Appl. Phys. Lett. 83 2124
[4] Esaki L and Tsu R 1970 I.B.M. J. Res. Dev. 14 61
[5] Ktitorov S A, Simin G S, and Sindalovski Y 1971 Fiz. Tverd Tela 13 2230 [1972 Sov. Phys. Solid State 13 1872]
[6] Savvidis P G, Kolasa B, Lee G, Allen S J 2004 Phys. Rev. Lett. 92 196802
[7] Shockley W 1954 Bell Syst. Tech. J. 33 799

[8] Kroemer H 1970 Proc. IEEE 58 1844
[9] Sze S M 1990 High-Speed Semiconductor Devices (New York: Wiley-Interscience)
[10] Ignatov A A, Piskarev V I and Shashkin V I 1985 Fiz. Tek. Pol. 19 2183 [1985 Sov. Phys. Semicond. 19 1345]
[11] Keay B J, Allen S J, Jr., Galan J, Kaminki J P, Campman K L, Gossard A C, Bhattacharya U, Rodwell M J W 1995 Phys. Rev. Lett. 75 4098
[12] Unterrainer K, Keay B J, Wanke M C, Allen S J, Leonard D, Medeiros-Ribeiro G, Bhattacharya U, Rodwell M J W 1996 Phys. Rev. Lett. 76 2973
[13] Tucker J R, 1979 IEEE J. Quantum Electron. QE-15 1234; Tucker J R and Feldman M J 1985 Rev. Mod. Phys. 57 1055
[14] Wacker A 2002 Physics Reports, 357 1